The ISME Journal (2008) 2, 615–631

www.nature.com/ismej

ORIGINAL ARTICLE

Escherichia coli transcription factor YncC (McbR) regulates colanic acid and biofilm formation by repressing expression of periplasmic protein YbiM (McbA)

Xue-Song Zhang[1], Rodolfo García-Contreras[1] and Thomas K Wood[1,2,3]
[1]*Artie McFerrin Department of Chemical Engineering, Texas A & M University, College Station, TX, USA;* [2]*Department of Biology, Texas A & M University, College Station, TX, USA and* [3]*Zachry Department of Civil Engineering, Texas A & M University, College Station, TX, USA*

Quorum-sensing signal autoinducer 2 (AI-2) stimulates *Escherichia coli* biofilm formation through the motility regulator MqsR that induces expression of the putative transcription factor encoded by *yncC*. Here, we show that YncC increases biofilm formation by repressing overproduction of the exopolysaccharide identified as colanic acid (corroborated by decreasing mucoidy and increased sensitivity to bacteriophage P1 infection). Differential gene expression and gel shift assays demonstrated that YncC is a repressor of the predicted periplasmic protein-encoding gene, *ybiM*, which was corroborated by the isogenic *yncC ybiM* double mutation that repressed the *yncC* phenotypes (biofilm formation, colanic acid overproduction, mucoidy and bacteriophage resistance). Through nickel-enrichment DNA microarrays and additional gel shift assays, we found that the putative transcription factor B3023 (directly upstream of *mqsR*) binds the *yncC* promoter. Overexpressing MqsR, AI-2 import regulators LsrR/LsrK and AI-2 exporter TqsA induced *yncC* transcription, whereas the AI-2 synthase LuxS and B3023 repressed *yncC*. MqsR has a toxic effect on *E. coli* bacterial growth, which is partially reduced by the b3023 mutation. Therefore, AI-2 quorum-sensing control of biofilm formation is mediated through regulator MqsR that induces expression of the transcription factor YncC. YncC inhibits the expression of periplasmic YbiM, which prevents overproduction of colanic acid (excess colanic acid causes mucoidy) and prevents YbiM from inhibiting biofilm formation.
The ISME Journal (2008) **2,** 615–631; doi:10.1038/ismej.2008.24; published online 28 February 2008
Subject Category: microbe-microbe and microbe-host interactions
Keywords: AI-2; biofilm; colanic acid; exopolysaccharide; gene expression; mucoidy

Introduction

Escherichia coli biofilm development is a complex process with at least five developmental stages; initial reversible attachment of planktonic cells to a solid surface, transition from reversible to irreversible attachment, early development of biofilm architecture, development of microcolonies into mature biofilm and dispersion of cells from the biofilm to return to the planktonic state (Van Houdt and Michiels, 2005). Hundreds of genes are differentially expressed during this biofilm development process (Schembri *et al.*, 2003; Beloin *et al.*, 2004; Ren *et al.*, 2004a) and bacterial signaling such as quorum and metabolite sensing and catabolite repression are involved in this process (Jackson *et al.*, 2002; Stanley and Lazazzera, 2004; Camilli and Bassler, 2006).

One recently-characterized metabolite biofilm signal is indole, which represses biofilm formation of *E. coli* by repressing motility, inducing the sensor of the quorum-sensing signal autoinducer-1 and influencing acid resistance (Lee *et al.*, 2007b). A series of genes including *bssR*/*bssS*, *bhsA* and *ariR* have been identified as regulating biofilm formation through indole (Domka *et al.*, 2006; Lee *et al.*, 2007c; Zhang *et al.*, 2007), and hydroxy indoles have been shown to be signals for pathogenic *E. coli* (Bansal *et al.*, 2007; Lee *et al.*, 2007a).

Another signal controlling the biofilm development of *E. coli* is autoinducer 2 (AI-2) (González Barrios *et al.*, 2006), a bacterial species-nonspecific signal used by both Gram-negative and Gram-positive bacteria and synthesized by

Correspondence: TK Wood, Chemical Engineering, Texas A & M University, 220 J. E. Brown Building, 3122 TAMU, College Station, TX 77843-3122, USA.
E-mail: thomas.wood@chemail.tamu.edu
Received 20 December 2007; accepted 11 February 2008; published online 28 February 2008

S-ribosylhomocysteine lyase (LuxS) (Schauder *et al.*, 2001). LuxS converts *S*-ribosyl-homocysteine into homocysteine and 4,5-dihydroxy-2,3-pentanedione (DPD), which cyclizes spontaneously into a family of AI-2 molecules (Lombardia *et al.*, 2006). As a bacterial communication signal, AI-2 is exported by TqsA (Herzberg *et al.*, 2006) and internalized by a *lsr* operon-encoded system (Taga *et al.*, 2003), and then controls a variety of genes (DeLisa *et al.*, 2001b; Xavier and Bassler, 2003; Ren *et al.*, 2004b). The *lsr* operon of seven genes *lsrACDBFGE* is induced by phospho-AI-2 and regulated by LsrR, LsrK and GlpDK (Taga *et al.*, 2001, 2003; Xavier and Bassler, 2005). The regulator LsrR represses the AI-2 uptake operon *lsr*, which is derepressed by the binding of phospho-AI-2 to LsrR (Taga *et al.*, 2003). Another regulator, LsrK, a cytoplasmic kinase, phosphorylates internal AI-2 into an activated molecule (Xavier and Bassler, 2005). The glycerol uptake and metabolism system encoded by *glpDFK* also influences AI-2 signaling by regulating *lsr* transcription through LsrR (Xavier and Bassler, 2005).

Some insights have been gained as to how AI-2 controls biofilm formation. In *E. coli*, AI-2 stimulates biofilm formation and changes its architecture by stimulating flagellar motility via the quorum-sensing regulator MqsR that acts through the two-component motility regulatory system QseBC (González Barrios *et al.*, 2006), which transcriptionally regulates FlhDC, the master regulator of flagella and motility genes *fliLMNOPQR, fliAZ*, *flhBA* and *flgABCDMN* (Liu and Matsumura, 1994; Claret and Hughes, 2002; Clarke and Sperandio, 2005). This result is consistent with the recent finding that in the oral bacterium *Aggregatibacter actinomycetemcomitans*, AI-2 regulates its biofilm formation most likely through its QseBC system (Shao *et al.*, 2007). Also, in the human gastric pathogen *Helicobacter pylori*, AI-2 controls motility by controlling genes upstream of the motility and flagellar regulator FlhA (Rader *et al.*, 2007). Further proof that AI-2 controls motility in different genera is that AI-2 regulates transcription of the flagellin gene, *flaA*, in the human pathogen *Campylobacter jejuni* (Jeon *et al.*, 2003). In addition, BssR/BssS regulate *E. coli* biofilms by influencing AI-2 and indole concentrations in a divergent manner (Domka *et al.*, 2006), and AI-2 regulates the dual-species biofilm formation of two Gram-positive human oral commensal bacterial strains, *Actinomyces naeslundii* T14V and *Streptococcus oralis* 34, at an optimum concentration (Rickard *et al.*, 2006).

Details of how MqsR functions are still not clear. MqsR was first shown to be highly induced in biofilms by Ren *et al.* (2004a). MqsR has also been reported to be a putative cyanide hydratase based on sequence similarity (Reed *et al.*, 2003) and to be a toxin protein of a toxin/antitoxin operon, which is the most induced gene in *E. coli* persister cells (Shah *et al.*, 2006). Differential expression analysis by DNA microarrays indicated that MqsR is a global regulator of *E. coli* gene expression (González Barrios *et al.*, 2006); for example, MqsR induces *flhDC* and *lsrK* and represses *glpDFK* (González Barrios *et al.*, 2006), which further supports the model of quorum-sensing regulation of biofilm through MqsR. In addition, the recognition that MqsR induces *ymgB* (González Barrios *et al.*, 2006) is consistent with the recent finding that this gene is critical for *E. coli* biofilm formation and acid resistance influenced by indole (Lee *et al.*, 2007c). Two uncharacterized putative transcription regulators, *yncC* (b1450) and *yiaG* (b3555), were also identified as induced by MqsR (González Barrios *et al.*, 2006). Also, *yncC* was identified as induced by deleting the AI-2 regulator genes *lsrR* and *lsrK* (Li *et al.*, 2007). Here, we show that YncC is important for *E. coli* biofilm formation, that YncC inhibits colanic acid overproduction and thereby inhibits mucoidy by repressing expression of periplasmic protein YbiM, and that YncC plays a key role in the regulation of biofilm formation by quorum-sensing regulator MqsR.

Materials and methods

Bacterial strains, plasmids, media and growth conditions

The strains and plasmids used in this study are listed in Table 1. *E. coli* K12 MG1655 was obtained from the *E. coli* Genome Project of the University of Wisconsin-Madison (Blattner *et al.*, 1997). *E. coli* K12 BW25113, its isogenic mutants and the pCA24N-based plasmids for expressing YncC, MqsR, B3023, LsrR, LsrK, LuxS and TqsA under the tight regulation via the $lacI^q$ repressor, were obtained from the Genome Analysis Project in Japan (Baba *et al.*, 2006). Expression of the target proteins from these plasmids was induced by isopropyl-β-D-thiogalactopyranoside (IPTG) (Sigma, St Louis, MO, USA). The expression vector plasmid pBAD-*Myc*-His C (Invitrogen, Carlsbad, CA, USA) was used to construct pBAD-*Myc*-His C-b3023. Expression of C-terminal histidine-tagged B3023 protein under the arabinose-inducible *araBAD* promoter (P_{BAD}) from this plasmid was induced by 0.5% L-arabinose (Acros Organics, Morris Plains, NJ, USA). The promoter-probe vector pPROBE-*gfp*[tagless] (Miller *et al.*, 2000) was used to construct pP*yncC-gfp*, which carries the *yncC* promoter-*gfp* fusion.

Luria–Bertani medium (LB) was used to preculture all the *E. coli* cells (Sambrook *et al.*, 1989) at 37 °C. LB medium was also used for bacterial growth rates, indole assays, green fluorescence protein (GFP) fluorescence intensity assays, the glass wool biofilm DNA microarrays and the nickel-enrichment DNA microarray experiments. To investigate the exopolysaccharide (EPS), bacterial strains were streaked on LB calcofluor plates (LB agar plates containing 100 μg ml^{-1} calcofluor

Table 1 Strains and plasmids used. Km^R, Cm^R and Amp^R are kanamycin, chloramphenicol and ampicillin resistance, respectively

Strain and plasmid	*Genotype/relevant characteristics*	*Source*
Strain		
E. coli K-12 BW25113	*lacI*^{q} *rrnB*$_{T14}$ *ΔlacZ*$_{WJ16}$ *hsdR514* *ΔaraBAD*$_{AH33}$ *ΔrhaBAD*$_{LD78}$	(Datsenko and Wanner, 2000)
E. coli K-12 BW25113 *yncC*	K-12 BW25113 Δ*yncC* Ω*Km*^{R}	(Baba *et al*., 2006)
E. coli K-12 BW25113 *ybiM*	K-12 BW25113 Δ*ybiM* Ω*Km*^{R}	(Baba *et al*., 2006)
E. coli K-12 BW25113 b3023	K-12 BW25113 Δb3023 Ω*Km*^{R}	(Baba *et al*., 2006)
E. coli K-12 BW25113 *wcaA*	K-12 BW25113 Δ*wcaA* Ω*Km*^{R}	(Baba *et al*., 2006)
E. coli K-12 BW25113 *wcaD*	K-12 BW25113 Δ*wcaD* Ω*Km*^{R}	(Baba *et al*., 2006)
E. coli K-12 BW25113 *luxS*	K-12 BW25113 Δ*luxS* Ω*Km*^{R}	(Baba *et al*., 2006)
E. coli K-12 MG1655	F$^-$ λ$^-$ *ilvG rfb-50 rph-1*	(Blattner *et al*., 1997)
E. coli K-12 MG1655 *yncC*	K-12 MG1655 Δ*yncC* Ω*Km*^{R}	This work
E. coli K-12 MG1655 *yncC Km*	K-12 MG1655 Δ*yncC* Δ*Km*^{R} (removed Km^R gene from MG1655 Δ*yncC* Ω*Km*^{R})	This work
E. coli K-12 MG1655 *ybiM*	K-12 MG1655 Δ*ybiM* Ω*Km*^{R}	This work
E. coli K-12 MG1655 *yncC ybiM*	K-12 MG1655 Δ*yncC* Δ*ybiM* Ω*Km*^{R}	This work
E. coli K-12 MG1655 *yncC wcaA*	K-12 MG1655 Δ*yncC* Δ*wcaA* Ω*Km*^{R}	This work
E. coli K-12 MG1655 *yncC wcaD*	K-12 MG1655 Δ*yncC* Δ*wcaD* Ω*Km*^{R}	This work
E. coli K-12 MG1655 *luxS*	K-12 MG1655 Δ*luxS* Ω*Km*^{R}	This work
E. coli K-12 MG1655 *luxS Km*	K-12 MG1655 Δ*luxS* Δ*Km*^{R} (removed Km^R gene from MG1655 Δ*yncC* Ω*Km*^{R})	This work
E. coli DH5α	*luxS supE44 ΔlacU169*(Φ80d*lacZ*ΔM15) *hsdR17 recA endA1 gyr96 thi-1 relA1*	(Ren *et al*., 2004b)
Plasmid		
pCA24N	Cm^R; *lacI*^{q}, pCA24N	(Baba *et al*., 2006)
pCA24N-*yncC*	Cm^R; *lacI*^{q}, pCA24N P$_{T5\text{-}lac}$::*yncC*$^+$	(Baba *et al*., 2006)
pCA24N-*mqsR*	Cm^R; *lacI*^{q}, pCA24N P$_{T5\text{-}lac}$::*mqsR*$^+$	(Baba *et al*., 2006)
pCA24N-b3023	Cm^R; *lacI*^{q}, pCA24N P$_{T5\text{-}lac}$::*b3023*$^+$	(Baba *et al*., 2006)
pCA24N-*tqsA*	Cm^R; *lacI*^{q}, pCA24N P$_{T5\text{-}lac}$::*tqsA*$^+$	(Baba *et al*., 2006)
pCA24N-*luxS*	Cm^R; *lacI*^{q}, pCA24N P$_{T5\text{-}lac}$::*luxS*$^+$	(Baba *et al*., 2006)
pCA24N-*crp*	Cm^R; *lacI*^{q}, pCA24N P$_{T5\text{-}lac}$::*crp*$^+$	(Baba *et al*., 2006)
pCA24N-*crl*	Cm^R; *lacI*^{q}, pCA24N P$_{T5\text{-}lac}$::*crl*$^+$	(Baba *et al*., 2006)
pCP20	Amp^R Cm^R; temperature-sensitive replication and thermal induction of FLP recombinase	(Cherepanov and Wackernagel, 1995)
pPROBE-*gfp*[tagless]	Km^R; Promoterless *gfp* vector plasmid	(Miller *et al*., 2000)
pP*yncC-gfp*	Km^R; P$_{yncC}$ ::*gfp* in pPROBE-*gfp*[tagless]	This work
pBAD-*Myc*-His C	Amp^R; *E. coli* L-arabinose inducible expression vector	Invitrogen
pBAD-*Myc*-His C-b3023	Amp^R; P$_{BAD}$::b3023 in pBAD-*Myc*-His C	This work

Abbreviation: *E. coli, Escherichia coli*.

(Sigma)) and also on LB Congo red plates (LB agar plate containing 20 μg ml^{-1} Congo red (Sigma) and 10 μg ml^{-1} Coomassie brilliant blue (Sigma)), incubated at 37 °C for 24–48 h and dye binding was evaluated by illuminating under UV light for calcofluor binding or by red color intensity for Congo red binding (Ferrieres *et al*., 2007).

Kanamycin (50 μg ml^{-1}) was used for pre-culturing the *E. coli* BW25113 or MG1655 isogenic knockouts. Kanamycin (100 μg ml^{-1}) was used for selecting plasmids pPROBE-*gfp*[tagless] and pP*yncC-gfp*. Chloramphenicol (30 μg ml^{-1}) was used for selecting plasmid pCP20 and the plasmids derived from pCA24N. Both kanamycin (100 μg ml^{-1}) and chloramphenicol (30 μg ml^{-1}) were used to select for MG1655 hosting two plasmids, pP*yncC-gfp* and a pCA24N-based plasmids. Ampicillin (100 μg ml^{-1}) was used for selecting plasmids pBAD-*Myc*-His C and pBAD-*Myc*-His C-b3023.

The specific growth rates of wild-type *E. coli* and the *yncC* mutant were determined by measuring the cell turbidity at 600 nm of two independent cultures of each strain as a function of time using values less than 0.7. Growth curves of the wild-type strain and the *yncC* mutant were obtained by measuring the cell turbidity at 600 nm of two independent cultures as a function of time until late stationary phase.

P1 transduction

Bacteriophage P1 transduction was used to construct mutants in MG1655 using BW25113-based mutants available from the KEIO collection (Baba *et al*., 2006). Briefly, to construct the MG1655 *yncC* Ω*Km*^{R} mutant with a complete deletion of *yncC* (*Km*^{R}: kanamycin-resistance marker gene), bacteriophage P1 was grown with BW25113 *yncC* Ω*Km*^{R}, and the lysate was used to transduce MG1655. Kanamycin-resistance colonies were selected, and the correct *yncC* Ω*Km*^{R} mutation in the MG1655 genome was confirmed by PCR using the forward locus-specific primer in the *yncC* upstream region 5′-GCAAAGTGGTGATCCGCG-3′ and the reverse kanamycin-specific primer K1, 5′-CAGTCATAGCC

GAATAGCCT-3′. To construct the MG1655 *yncC ybiM* double mutation, the kanamycin-resistance gene was deleted from MG1655 *yncC* ΩKm^R by introducing plasmid pCP20, which expresses the FLP recombinase to eliminate kanamycin-resistance selective marker (Cherepanov and Wackernagel, 1995), by curing the plasmid by 43 °C incubation and by selecting kanamycin-sensitive and chloramphenicol-sensitive colonies of MG1655 *yncC* Km^R that lack pCP20 (Datsenko and Wanner, 2000). The *ybiM* ΩKm^R mutation was then introduced into the MG1655 *yncC* Km^R mutant from BW25113 *ybiM* of the KEIO collection (Baba *et al.*, 2006) by bacteriophage P1 transduction, which led to the construction of the double mutant MG1655 *yncC ybiM* ΩKm^R. The correct *ybiM* ΩKm^R mutation in the MG1655 *yncC ybiM* ΩKm^R genome was confirmed by PCR using the forward locus-specific primer in the *ybiM* upstream region, 5′-GCAAAGTGGTGATCCGCG-3′, and the reverse, kanamycin-specific primer K1. The double mutants MG1655 *yncC wcaA* ΩKm^R, and *yncC wcaD* ΩKm^R were constructed in the same way. The correct *wcaA* ΩKm^R, and *wcaD* ΩKm^R mutation in each double mutant was confirmed by PCR using a forward locus-specific primer, 5′-GGTCGTC ATGTCGGAACCAC-3′ or 5′-CTCAATCAGATGGA TGCGCT-3′, respectively, and the common reverse, kanamycin-specific primer K1. In a similar way, the MG1655 *luxS* Km^R mutant was constructed by introducing the *luxS* ΩKm^R mutation into the MG1655 wild-type strain from BW25113 *luxS* of the KEIO collection by bacteriophage P1 transduction to construct mutant MG1655 *luxS* ΩKm^R, and the kanamycin-resistance gene was deleted from MG1655 *luxS* ΩKm^R as described above.

Construction of plasmids

To construct a *yncC* promoter-*gfp* reporter fusion, a 323 bp DNA fragment containing the *yncC* promoter region (from 306 bp to 1 bp upstream of *yncC* start codon) was obtained by PCR using the BW25113 genome as the template and the pair of primers, 5′-CG CGGATCCGCGAAGAAATTACTGACGGT-3′ and 5′-G GGGAGCTCTTTAATTCCTTCGCGTGTTT-3′, which also inserted restriction sites, *Bam*HI and *Sac*I, upstream and downstream of the *yncC* promoter, respectively. After double digestion with restriction enzymes, *Bam*HI and *Sac*I, the DNA fragment was cloned into the promoter-probe vector plasmid pPROBE-*gfp*[tagless] (Miller *et al.*, 2000), which led to the plasmid pP*yncC-gfp*.

To construct a plasmid expressing C-terminal histidine-tagged B3023 protein for the nickel-enrichment DNA microarrays, a 495 bp DNA fragment containing the b3023 gene was obtained by PCR using the BW25113 genome as a template and the pair of primers, 5′-AGCTCGAGAACAAACCT-GACACTGGATGT-3′ and 5′-GTAAGCTTCCGCCAA CGGCACATAAACAT-3′; this DNA fragment was cloned into expression vector pBAD-*Myc*-His C (Invitrogen), to form plasmid pBAD-*Myc*-His C-b3023, which expresses the C-terminal histidine-tagged B3023 under the L-arabinose-inducible P_{BAD} promoter.

Crystal-violet biofilm assay

A static biofilm formation assay was performed in 96-well polystyrene plates as reported previously (Ren *et al.*, 2005). Briefly, cells were inoculated with an initial turbidity at 600 nm of 0.05 in LB or LB glu at 37 °C or 30 °C for 24 h without shaking, then cell density (turbidity at 620 nm) and total biofilm (absorbance at 540 nm) were measured using crystal violet staining. Total biofilm (air/liquid and liquid/plastic interface) was normalized by bacterial growth for each strain. Each data point was averaged from at least 12 replicate wells (6 wells from each of the two independent cultures).

Indole assay

Extracellular, stationary-phase, planktonic indole concentrations of MG1655 and MG1655 *yncC* cultured in LB at 37 °C with shaking (250 r.p.m.) were measured spectrophotometrically as described previously (Domka *et al.*, 2006) at 7, 15 and 24 h. Each experiment was performed with two independent cultures for each strain.

EPS and colanic acid assays

To quantify the total EPS, approximately 60 mg of mucoid or non-mucoid bacterial culture was collected from the surface of LB agar plates after a 12-h incubation at 37 °C, and then thoroughly resuspended in 1 ml sterile distilled water by vortex. The cell concentration was determined by cell turbidity at 600 nm. To inactivate EPS-degrading enzymes and to completely release EPS from the cell surface, the resuspended culture was boiled for 10 min. After cooling to room temperature, each sample was centrifuged at 16 000 *g* for 10 min, and the supernatant fraction was saved at −20 °C for quantification. The anthrone-H_2SO_4 assay was used to quantify total EPS as previously described based on quantification of glucose equivalents in the EPS (Mendrygal and González, 2000). Briefly, each 0.4 ml suitably-diluted sample was mixed with 0.1 ml of fresh 2% anthrone (Acros Organics) in ethyl acetate (Acros Organics) in a 10 ml glass test tube. One milliliter of 95–97% H_2SO_4 (Acros Organics) was added into each sample slowly, and the reactions were cooled for 10 min to room temperature, then the value of the absorbance at 620 nm of each reaction product was determined. Glucose equivalents in the EPS samples were quantified using a calibration curve with glucose (Sigma) from 10 to 80 $\mu g\,ml^{-1}$, and the values were normalized by cell turbidity at 600 nm. All experiments were performed with two independent cultures.

Colanic acid from bacterial colonies was assayed by measuring fucose, the specific sugar component of this EPS (Obadia *et al.*, 2007), according to the method of Obadia *et al.*, (2007), which is based on the specific difference in absorbance at 396 and 427 nm after reacting fucose with sulfuric acid and cysteine hydrochloride. A *L*-fucose (Acros Organics) calibration curve was used (10–60 $\mu g\,ml^{-1}$) to determine the fucose concentration, and these values were normalized by cell turbidity at 600 nm. All experiments were performed with two independent cultures. As a negative control, glucose was assayed and found to not produce a significant signal (as low as that using distilled water that lacked fucose); hence, the assay is specific to colanic acid.

P1 phage infection sensitivity assay

The bacteriophage infection sensitivity assay was performed as described before (Ho and Waldor, 2007) with the following modification. An overnight culture (12 h) was centrifuged (1500 *g*) for 5 min, and resuspended in LB to a turbidity of 3 at 600 nm. A serial of dilution of the P1 phage was prepared (10^0, 10^{-1}, 10^{-2}, 10^{-3}, 10^{-4} and 10^{-5}). A 0.01 ml volume of each serial dilution of the P1 phage was mixed with 0.1 ml of cell culture and incubated for 10 min at 37 °C. The cells were pelleted by centrifugation (1500 *g*) for 5 min to remove unattached phage, resuspended in 0.1 ml LB, mixed with 3 ml of the top agar (LB with 5 mM $CaCl_2$, and 0.7% agar, kept at 50 °C) and then poured onto a standard LB plate. After solidification, the plates were incubated at 37 °C overnight, and then plaques were counted based on suitable phage dilution. Two independent cultures were used for all the experiments.

GFP fluorescence intensity assay

The specific GFP fluorescence intensity of cell cultures were found by diluting each culture quickly with phosphate-buffered saline (PBS, NaCl 8 $g\,l^{-1}$, KCl 0.2 $g\,l^{-1}$, Na_2HPO_4 1.44 $g\,l^{-1}$ and KH_2PO_4 0.24 $g\,l^{-1}$, pH 7.4) (Sambrook *et al.*, 1989) in 96-well plates to a turbidity of 0.1–0.2 at 600 nm. The intensity of GFP fluorescence was quantified with a Spectra Max Germini EM fluorescence microplate reader (Molecular Devices, Sunnyvale, CA, USA) using an excitation wavelength of 485 nm, an emission wavelength of 528 nm and a cutoff wavelength of 515 nm. The cell turbidity was quantified at 600 nm with a Sunrise microplate reader (Tecan, Austria Gesellschaft, Salzburg, Austria), and the GFP fluorescence intensity of each of the cell suspensions was normalized by its cell density. The promoter-less GFP strain MG1655/pPROBE-*gfp*[tagless] was used as the negative control. Two independent cultures were used for the experiments.

Total RNA isolation and DNA microarrays

DNA microarray experiments were performed to examine differential gene expression in biofilm cells upon deleting *yncC* in two independent ways as follows: (i) *E. coli* K-12 MG1655 *yncC* colony cells were grown on LB agar plates at 37 °C for 15 h as there was a clear phenotype of mucoidy vs the wild-type strain, and (ii) *E. coli* BW25113 *yncC* biofilm cells were developed on glass wool at 37 °C for 15 h. For the agar biofilm, fresh single colonies of wild-type *E. coli* MG1655 and MG1655 *yncC* were re-streaked on LB agar plates, incubated and about 0.05 g of the colony cultures on an LB plate were quickly transferred to 2-ml collection tubes. The total RNA was isolated from these colony cells as described previously (Ren *et al.*, 2004a). The *E. coli* GeneChip Genome 2.0 Array (Affymetrix, P/N 900551, Santa Clara, CA, USA) containing 10 208 probe sets for open reading frames, rRNA, tRNA and intergenic (IG) regions for four *E. coli* strains: MG1655, CFT073, O157:H7-Sakai and O157:H7-EDL933, was used to analyze the complete *E. coli* transcriptome.

For the glass wool biofilm, overnight cultures (16 h, 2.5 ml) of wild-type *E. coli* BW25113 and BW25113 *yncC* in LB and LB with kanamycin (50 $\mu g\,ml^{-1}$), respectively, were used to inoculate 250 ml LB with 10 g of glass wool (Corning Glass Works, Corning, NY, USA) for forming biofilm (Ren *et al.*, 2004a). After incubating at 37 °C for 15 h with shaking (250 r.p.m.), biofilm cells were prepared by rinsing and sonicating the glass wool in sterile 0.85% NaCl solution at 0 °C as described before (Zhang *et al.*, 2007). The total RNA was isolated from biofilm cells as described previously (Ren *et al.*, 2004a). The *E. coli* Genechip antisense genome array (P/N 900381, Affymetrix) containing probes for more than 4200 open reading frames was used to analyze the complete *E. coli* transcriptome as described previously (Zhang *et al.*, 2007).

For both sets of microarrays, hybridization was performed for 16 h, and the total cell intensity was scaled to an average value of 500. The probe array images were inspected for any image artifact. Background values, noise values and scaling factors of both arrays were examined and were comparable. The intensities of polyadenosine RNA control were used to monitor the labeling process. As expected, signals of the deleted genes, *araA* and *rhaA,* were low for both BW25113 and BW25113 *yncC*, whereas the signals of *yncC* were low for the *yncC* mutants for both BW25113 and MG1655. For both sets of binary microarray comparisons to determine differential genes expression, if the gene with the larger transcription rate did not have a consistent transcription rate based on the 11–15 probe pairs (*P*-value less than 0.05), these genes were discarded. A gene was considered differentially expressed when the *P*-value and the corrected *P*-value based on the False Discovery Rate Method (Benjamini and Hochberg, 1995) for comparing two

chips were lower than 0.05 (to assure that the change in gene expression was statistically significant and that false positives arise less than 5%) and when the expression ratio was higher than the s.d. for all of the *E. coli* K-12 genes (1.6-fold for both) (Ren *et al.*, 2004b). The gene functions were obtained from the National Center for Biotechnology Information database (Wheeler *et al.*, 2006), and the EcoCyc database (Keseler *et al.*, 2005).

Nickel-enrichment DNA microarrays

Overnight cultures of *E. coli* K-12 BW25113 carrying pBAD-*Myc*-His C or pBAD-*Myc*-His C-b3023 cells were diluted (1:100) into 250 ml LB with ampicillin (100 μg ml^{-1}). The cultures were grown to a turbidity of 0.8 at 600 nm at 37 °C with shaking (250 r.p.m.), and then were kept at 4 °C for 45 min to stop growth. L-arabinose (final concentration of 0.5%) was added to induce the synthesis of C-terminal histidine-tagged B3023 protein from pBAD-*Myc*-His C-b3023. The cultures were incubated overnight at room temperature with shaking (160 r.p.m.). Formaldehyde (1%, Fisher, Fair Lawn, NJ, USA) was applied to promote crosslinking between the C-terminal histidine-tagged B3023 protein and the DNA to which it was bound (Tamimi *et al.*, 2004), and the cultures were incubated for another 20 min with shaking (100 r.p.m.) at room temperature. Glycine (0.125 M, Sigma) was applied to stop the crosslinking for 5 min with shaking (100 r.p.m.). The cells were collected, washed with 200 ml of cold sodium chloride-phosphate (0.5 M NaCl, 50 mM NaH_2PO4, pH 8) buffer and resuspended in 25 ml of the same buffer with 1 mM phenylmethylsulfonyl fluoride (Pierce Biotechnology, Rockford, IL, USA). The cells were lysed by a French press (Thermo Electron Corp., San Jose, CA, USA), and the lysate was centrifuged at 12 000 *g* force at 4 °C for 20 min to remove the cellular debris. Ni-NTA agarose gel resin was used to bind the C-terminal His_6-tagged B3023-DNA complexes. The eluate with B3023-DNA complexes was treated with 75 μg ml^{-1} RNase A and 100 μg ml^{-1} proteinase K. The RNA and protein-free DNA fragments were then purified, and the presence of DNA fragments of 100–1000 bp was confirmed by gel electrophoresis. The DNA fragments were labeled with biotin at 3′-end, and the protein/RNA-free DNA samples were prepared for microarray analysis as described previously (Lee *et al.*, 2007c). The DNA fragments were labeled and DNA microarrays were performed using *E. coli* Genechip antisense genome array (P/N 900381, Affymetrix) (Ren *et al.*, 2004a). For analysis of the data, we chose as positive candidate IG regions with a signal greater than 1000 and at least eightfold enriched compared to the non-B3023 control array (empty vector pBAD-*Myc*-His C) as the global average signal of all the genes and IG regions in the B3023 chip was 588 and the s.d. of the enrichment (B3023 chip signal compared to the empty vector signal) was 5.

Electrophoretic mobility shift assay

Electrophoretic mobility shift assays (EMSA) were performed as described previously (Zhang *et al.*, 2007). To identify the promoter regions YncC binds, YncC was synthesized using the EasyXpress Linear Template Kit Plus (Qiagen, Valencia, CA, USA). Promoters lie at a variable distance upstream of their associated start codons, but in a well-defined window upstream of the gene transcription start sites (Gordon *et al.*, 2006). In this work, we choose the region 200–300 bp upstream of the start codon of the associated genes as the promoter region, and five DNA fragments of these regions were amplified by PCR from genomic DNA of wild-type BW25113. The *ybiM* promoter region (262 bp, consisting of 233 bp of upstream and 29 bp downstream of the start codon of *ybiM*) was amplified by PCR with the primers 5′-CGACAGGGTAAATATCTG-3′ and 5′-GCAATCAGTAGTGTGAGG-3′. The *ybeL* promoter region (243 bp, consisting of 205 bp of upstream and 38 bp downstream of the start codon of *ybeL*) was amplified by PCR with primers 5′-CTACA AATGTAGCGTTGA-3′ and 5′-GCAACCAGTTC ACGGTAA-3′. The *yebT* promoter region (262 bp, consisting of 225 bp of upstream and 37 bp downstream of the start codon of *yebT*) was amplified by PCR with primers 5′-GCCAGCAAGGTTTACGCA-3′ and 5′-GCGCTTCAGTCGTCGAAG-3′. The *sfsA* promoter region (301 bp, consisting of 253 bp of upstream and 48 bp downstream of the start codon of *sfsA*) was amplified by PCR with primers 5′-GCT TAATCCAGCTGGCGA-3′ and 5′-GTAACGCTGAAT TAGCGT-3′. The *uspF* promoter region (272 bp, consisting of 231 bp of upstream and 41 bp downstream of the start codon of *uspF*) was amplified by PCR with primers 5′-CAACCTGTTGGATGAAGA-3′ and 5′-GAATCGGAAATATCGATA-3′. The PCR products were gel purified with a QIAquick Gel Extraction Kit (Qiagen) and then labeled with biotin using the Biotin 3′-end DNA Labeling Kit (Pierce Biotechnology). For the binding reaction, *in vitro*-synthesized YncC (0.5 μl out of total 25 μl product in the *in vitro*-translation system) was incubated with biotin-labeled target promoter (8 ng) and the non-specific competitor DNA (poly dI · dC, 1 μg) in a 20 μl binding reaction system supplied by the EMSA kit at room temperature for 15 min. For the competition assay, unlabeled promoter regions from 200 ng to 1 200 ng were used to confirm the specificity of protein-DNA binding. After the binding reaction, electrophoresis was conducted at 100 V for 2.5 h at 4 °C using a 6% DNA retardation gel (Invitrogen), then the samples were transferred to a nylon membrane (Roche Diagnostics GmbH, Mannheim, Germany) using a Mini Trans-Blot Electrophoretic Transfer Cell (Bio-Rad Laboratories, Hercules, CA, USA), and 3′-biotin-labeled DNA was detected with the Light-Shift Chemiluminescent EMSA kit (Pierce Biotechnology). Each experiment was performed twice.

Similarly, to identify the promoter regions B3023 protein binds, B3023 was synthesized. Four DNA

fragments of promoter regions, the fragment with the *yncC* promoter (IG953), the fragment with the *yiaT* and *yiaU* promoters (IG2314), the fragment with the *ssrS* promoter (IG1895) and the fragment with the *rybA* and *mntR* promoters (IG543), were amplified by PCR from genomic DNA of the wild-type strain BW25113. The *yncC* promoter region (278 bp, consisting of 232 bp of upstream and 46 bp downstream of the start codon of *yncC*) was amplified by PCR with the primers 5′-GC AAAGTGGTGATCCGCG-3′ and 5′-CCTGCAGAGTCA AACTGA-3′. The *yiaT* and *yiaU* promoter regions (242 bp, consisting of 180 bp of upstream and 62 bp downstream of the start codon of *yiaT*) was amplified by PCR with primers 5′-GCAGTTGCGCTTGCCATA-3′ and 5′-GGCAGCGATTACCGAGAT-3′. The small RNA *ssrS* promoter region (279 bp, 3, 053, 876–3, 054, 154 on the *E. coli* K-12 chromosome) (Keseler *et al.*, 2005) was amplified by PCR with primers 5′-GCGTATTCGG ATGCTGCA-3′ and 5′-CCTTGAACCCTTGGTTCA-3′. The small RNA *rybA* and *mntR* promoter region (263 bp, 852, 154–852, 416) was amplified by PCR with primers 5′-CAGCATTAACCGTACTTT-3′ and 5′-GCGACGACTCATTGTGCT-3′.

Microarray data accession number
The expression data have been deposited in the NCBI Gene Expression Omnibus (GEO) (http://www.ncbi.nlm.nih.gov/geo/) and are accessible through GEO series accession number GSE8706 (Edgar *et al.*, 2002).

Results

Deletion of yncC *decreases biofilm formation*
To investigate whether YncC controls biofilm formation, biofilm formation of the *yncC* deletion mutant was measured using the 96-well crystal-violet assay in LB at 37 °C. Growth-normalized biofilm formation of MG1655 *yncC* decreased 2.2 ± 0.5-fold in LB medium at 37 °C after 24 h compared to that of wild-type MG1655 (Figure 1). This biofilm defect was complemented by expressing *yncC* from plasmid pCA24N-*yncC* in MG1655 *yncC* using 0.1 mM IPTG since biofilm formation increased significantly (Figure 1). In addition, on deleting *yncC*, biofilm formation was reduced 1.9 ± 0.4-fold in LB glu medium (LB medium supplemented with 0.2 % (m/v) glucose) at 37 °C, was reduced 2.3 ± 0.5-fold in LB glu at 30 °C and was reduced 1.7 ± 0.3-fold in LB at 30 °C (Figure 1). As biofilm formation is dynamic, we examined its formation as a function of time on deleting *yncC*, and found biofilm decreased 2.5 ± 0.3-, 3.0 ± 0.4-, 2.2 ± 0.3- and 1.8 ± 0.3-fold in LB medium at 37 °C after 7, 15, 24 and 48 h of incubation, respectively.

Deletion of yncC *increases extracellular indole*
On deleting *yncC* in MG1655, the extracellular concentration of the biofilm signal indole increased

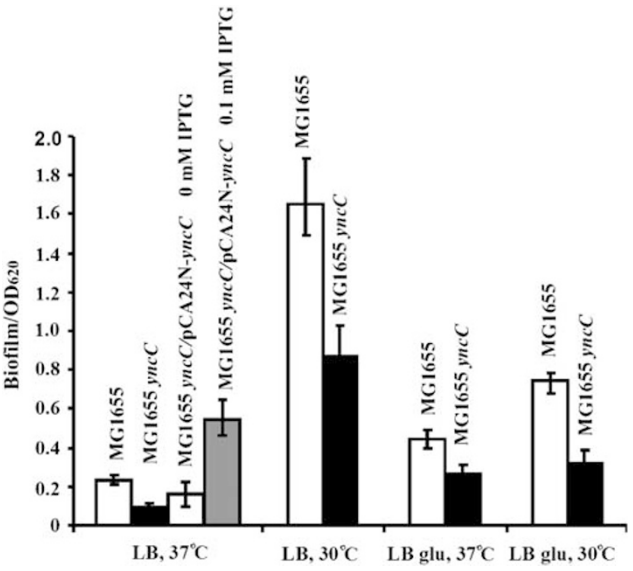

Figure 1 Total biofilm (air/liquid and liquid/plastic interface) normalized by bacterial growth (turbidity at 620 nm) after 24 h of incubation in LB or LB glu at 37 or 30 °C for the wild-type MG1655 and the mutant MG1655 *yncC* strains. Each experiment was performed in duplicate, and one s.d. is shown. LB, Luria–Bertani medium.

1.7 ± 0.2-, 2.1 ± 0.1- and 1.5 ± 0.2-fold after 7, 15 and 24 h in LB medium at 37 °C, respectively. Since indole acts as an extracellular signal that represses biofilm formation in *E. coli* K-12 (Domka *et al.*, 2006; Lee *et al.*, 2007b), the increase of extracellular indole concentration by deleting *yncC* is consistent with the observation that the *yncC* mutation decreased biofilm formation in LB medium.

Deletion of yncC *elicits mucoidy*
The MG1655 *yncC* culture became noticeably mucoid compared to the wild-type strain on LB agar (Figure 2a). As excessive production of bacterial EPS is a common cause of mucoidy in *E. coli* and other Gram-negative bacteria (Zinkewich-Peotti and Fraser, 1988; Qiu *et al.*, 2007), we collected EPS from mucoid MG1655 *yncC* culture and evaluated bacterial EPS production using an anthrone-H_2SO_4 assay. The normalized EPS from the mucoid MG1655 *yncC* culture was 10 ± 4-fold higher than that from the non-mucoid wild-type MG1655 culture. Therefore, *yncC* mutation leads to EPS overproduction and elicits mucoidy.

We also noticed that bacteriophage P1-mediated transduction using the strain MG1655 carrying the *yncC* mutation had a dramatically lower efficiency compared to using wild-type MG1655; deleting *yncC* from MG1655 increased bacteriophage P1 resistance 52 ± 16-fold compared to the wild-type MG1655. This result confirms that YncC represses EPS production as EPS overproduction increases bacteriophage P1 resistance by masking phage receptors on the bacterial surface thereby blocking phage infection (Petty *et al.*, 2007).

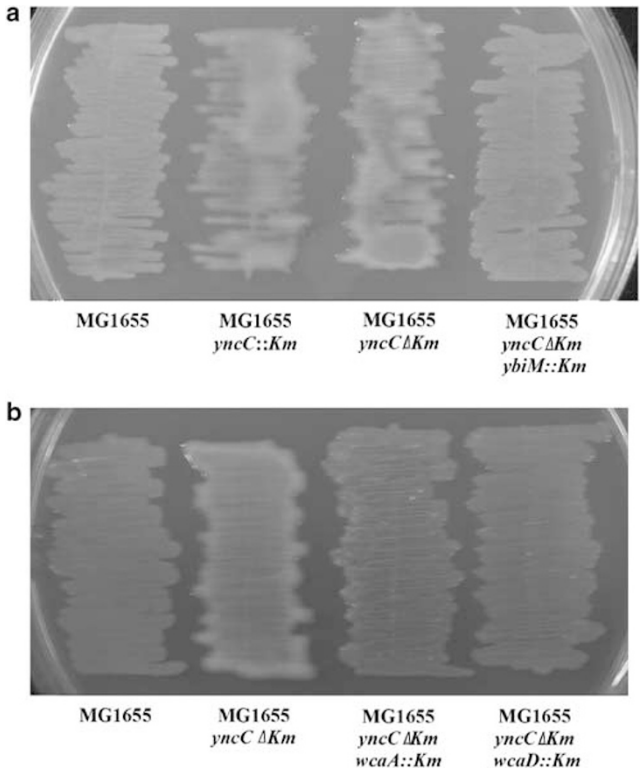

Figure 2 *Escherichia coli* MG1655 mutant *yncC* ΩKm^R and MG1655 *yncC* ΔKm^R cultures exhibit mucoidy on Luria–Bertani (LB) agar plates after 16 h of incubation at 37 °C, whereas the wild-type MG1655 and the double mutant MG1655 *yncC ybiM* ΩKm^R cultures lack mucoidy (**a**). *E. coli* MG1655 *yncC* ΔKm^R cultures exhibit mucoidy on LB agar plates after 16 h incubation at 37 °C, whereas wild-type MG1655 and the double mutants MG1655 *yncC wcaA* ΩKm^R and MG1655 *yncC wcaD* ΩKm^R cultures lack mucoidy (**b**).

Mucoidy is from overproduction of colanic acid

As colanic acid is an EPS that is commonly found in *E. coli* (Stevenson *et al.*, 1996), and as we have found its synthesis is controlled in a temporal manner in biofilms (Domka *et al.*, 2007) and is related to AI-2 signaling (Herzberg *et al.*, 2006), we investigated colanic acid production of MG1655 *yncC* mutant and the wild-type MG1655 strain by measuring fucose, which is a specific component of this EPS (Obadia *et al.*, 2007). Under the same conditions, the normalized colanic acid from the mucoid MG1655 *yncC* colonies was 326 ± 173-fold higher than that from the non-mucoid MG1655 colonies. Therefore, colanic acid is the overproduced EPS caused by the *yncC* mutation, and YncC inhibits *E. coli* colanic acid overproduction and thereby represses mucoidy.

To confirm these results, we deleted the colanic acid generation genes *wcaA* and *wcaD* along with *yncC* from MG1655 and investigated mucoidy in for the double mutants *wcaA yncC* and *wcaD yncC*. The deletion of either colanic acid gene dramatically repressed the MG1655 *yncC* mucoidy phenotype (Figure 2b); hence, YncC inhibits colanic acid overproduction.

To see if other types of EPS are overproduced by deleting *yncC*, EPS-calcofluor and EPS-Congo red binding tests were performed. Calcofluor as a fluorochrome binds to (1→3)-β- and (1→4)-β-D-glucopyranosides such as those found in cellulose, chitin and succinoglycans (Da Re and Ghigo, 2006). Congo red, along with binding curli, also binds (1→4)-α-D-glucopyranosides and basic or neutral EPS (Ferrieres *et al.*, 2007). However, both MG1655 *yncC* and wild-type MG1655 failed to bind calcofluor, which is consistent with previous reports for some other *E. coli* K12 MG1655 strains (Da Re and Ghigo, 2006), and both MG1655 *yncC* and wild-type MG1655 had the same Congo red-staining levels. These observations suggest that only colanic acid was overproduced by deleting *yncC*, whereas other EPS, such as cellulose, chitin, succinoglycans, Congo red-binding basic EPS or neutral EPS, were not overproduced by deleting *yncC*.

Genes regulated by YncC in biofilms

Whole-transcriptome analysis indicated that deletion of *yncC* induced 30 genes (Table 2) and repressed 10 genes more than fourfold in glass wool biofilm cells (Table 3). Among the most induced genes, *ptsH* (4.0-fold) encodes a heat-stable histidyl phosphorylatable protein (Postma *et al.*, 1993) that is induced by BssR/BssS in biofilms (Domka *et al.*, 2006). Also induced was *cpxP* (4.6-fold) that encodes a periplasmic adaptor protein involved in resistance to extracytoplasmic stress (Danese and Silhavy, 1998), which was induced in *E. coli* TG1 and TG biofilms (Beloin *et al.*, 2004) and is involved in adhesion of *E. coli* (Otto and Silhavy, 2002). *sixA* was induced 4.0-fold and encodes a signal inhibitory factor-X (Ogino *et al.*, 1998) that was induced in *E. coli* TG1 and TG biofilms (Beloin *et al.*, 2004). *fldA* was induced 5.3-fold and encodes flavodoxin 1 (Puan *et al.*, 2005) that was induced in the human urine biofilms of the asymptomatic *E. coli* bacteriuria strains (Hancock and Klemm, 2007).

Several poorly characterized genes were also induced on deletion of *yncC* including *ynhG* (4.6-fold), which was repressed in *E. coli* MG1655 biofilms (Schembri *et al.*, 2003), *ybiM* (6.5-fold), which was induced by AI-2 in *E. coli* W3110 (DeLisa *et al.*, 2001b), *yqjC* (4.6-fold), which was repressed by AI-2 in *E. coli* W3110 (DeLisa *et al.*, 2001b) and *yahO* (5.7-fold), which was induced by MqsR expression in *E. coli* MG1655 (González Barrios *et al.*, 2006).

Among the most repressed genes on deletion of *yncC* in biofilm cells (Table 3), *yceK* was repressed 4.0-fold and encodes a lipoprotein that is repressed in *E. coli* JM109 biofilms (Ren *et al.*, 2004a). Also repressed was *motB* (4.6-fold) that encodes a flagellar motor rotation protein whose mutation causes severe defects in biofilm formation (Pratt and Kolter, 1998). *yebT* was repressed 5.6-fold and encodes a putative outer membrane protein that was

Table 2 *Escherichia coli* genes were induced more than fourfold ($P<0.05$) upon deleting *yncC* in a BW25113 biofilm developed on glass wool for 15 h in LB at 37 °C

Gene	*b number*	*Expression ratio*	*Description*
Regulator			
sfsA[a,b]	b0146	6.1	Predicted DNA-binding transcriptional regulator of maltose metabolism
raiA (yfiA)[b]	b2597	4.9	Stationary phase translation inhibitor and ribosome stability factor
iscR	b2531	4.3	Iron-sulfur cluster transcription regulator
Adaptation			
dinJ	b0226	5.7	Predicted antitoxin of YafQ-DinJ toxin-antitoxin system
himD	b0912	5.7	Integration host factor (IHF), β subunit; site-specific recombination
uspF (ynaF)[a]	b1376	5.7	Stress-induced protein
glnH	b0811	5.3	Periplasmic glutamine-binding protein; permease
cpxP	b3913	4.6	Periplasmic adaptor protein, regulator of the Cpx response and possible chaperone involved in resistance to extracytoplasmic stress
clpS (yljA)	b0881	4.3	Specificity factor for ClpA-ClpP, ClpS shows OxyR-dependent induction of expression by hydrogen peroxide chaperone-protease complex
msyB	b1051	4.3	Acidic protein suppresses mutants lacking function of protein export
groS	b4142	4.3	GroES, 10 kDa chaperone binds to Hsp60 in pres. Mg-ATP, suppressing its ATPase activity
argT	b2310	4.0	Lysine-, arginine-, ornithine-binding periplasmic protein
sixA	b2340	4.0	Signal inhibitory factor-X, Phosphohistidine phosphatase affecting ArcB H-D phosphorelay; expression of six A is dependent on the alternative sigma factor *rpoE*
ptsH	b2415	4.0	PTS heat stable, histidyl phosphorylatable protein
dppA[b]	b3544	4.0	Dipeptide transport protein
Metabolism			
fldA	b0684	5.3	Flavodoxin 1
acpP	b1094	4.3	Acyl carrier protein
glgS	b3049	4.3	Predicted glycogen synthesis protein, *rpoS* dependent
ivbL	b3672	4.3	*ilvB* operon leader peptide
acs	b4069	4.0	Acetyl-CoA synthetase
RNA			
rpsV[b]	b1480	4.6	30S ribosomal subunit protein S22
Unknown function			
ybeL[a]	b0643	6.5	Putative alpha helical protein
ybiM[a,b]	b0806	6.5	Predicted periplasmic protein, YhcN family
yjfO	b4189	5.7	Probable lipoprotein, YhcN family
yahO	b0329	4.9	Predicted periplasmic protein, YhcN family
ydiZ[b]	b1724	4.9	Hypothetical protein
yoaC	b1810	4.9	Hypothetical protein
yjdN[b]	b4107	4.9	Hypothetical protein
yacL	b0119	4.6	Hypothetical protein
ybaA	b0456	4.6	Hypothetical protein
ycfP	b1108	4.6	Hypothetical protein
ynhG	b1678	4.6	Hypothetical protein
yqjC	b3097	4.6	Hypothetical protein
yegP	b2080	4.3	Hypothetical protein
yobF	b1824	4.0	Hypothetical protein
smg	b3284	4.0	Hypothetical protein

Abbreviation: LB, Luria–Bertani medium.
[a]Genes studied by a gel shift experiment with YncC.
[b]Genes also identified with MG1655 *yncC* cells developed on agar plates for 15 h in LB at 37 °C.

induced previously by LuxS (Wang *et al.*, 2005). Other highly-repressed genes include *hyfD* (4.3-fold), which encodes a hydrogenase membrane subunit (Andrews *et al.*, 1997), *frlA* (3.0-fold), which encodes a fructoselysine transporter (Wiame *et al.*, 2002) and *yieL* (7.0-fold), which encodes a putative xylanase; all three loci are repressed in LB glu biofilms by the AI-2 exporter TqsA (Herzberg *et al.*, 2006). Finding differential expression of these biofilm-related genes on deletion of *yncC* supports

Table 3 *Escherichia coli* genes were repressed more than threefold ($P<0.05$) upon deleting *yncC* in a BW25113 biofilm developed on glass wool for 15 h in LB at 37 °C

Gene	*b number*	*Expression ratio*	*Description*
Adaptation			
yebT [a]	b1834	−5.6	Putative outer membrane protein
motB	b1889	−4.6	Enables flagellar motor rotation, linking torque machinery to cell wall
yceK	b1050	−4.0	Novel verified lipoprotein
lomR_1 [b]	b1369	−3.2	Outer membrane protein interrupted by IS5Y
Metabolism			
yieL	b3719	−7.0	Putative xylanase
rutD	b1009	−4.6	α/β-hydrolase, pyrimidine utilization
proW	b2678	−4.6	High-affinity transport system for glycine betaine and proline
hyfD	b2484	−4.3	Hydrogenase 4 membrane subunit
hyfB	b2482	−3.5	Hydrogenase 4, component B
yjgI	b4249	−3.2	Putative oxidoreductase
agaW	b3134	−3.2	PTS system *N*-acetylgalactosamine-specific IIC component 2
ypdF	b2385	−3.0	Putative metalloenzyme with aminopeptidase activity
frlA (yhfM)	b3370	−3.0	Predicted fructoselysine transporter
dgoK	b3693	−3.0	2-oxo-3-deoxygalactonate kinase
RNA			
ileX	b3069	−6.1	Isoleucine tRNAs
argW	b2348	−5.3	Arginine tRNA5
Unknown function			
yagQ	b0283	−4.0	Hypothetical protein
yafX	b0248	−3.0	Hypothetical protein

Abbreviation: LB, Luria–Bertani medium.
[a]Studied by a gel shift experiment with YncC.
[b]Genes also identified with MG1655 *yncC* cells developed on agar plates for 15 h in LB at 37 °C.

that YncC plays an important role in the regulation of *E. coli* biofilm formation.

Seven of the most-induced genes on deleting *yncC* in biofilm cells were also induced on deleting *yncC* in colony cells from LB agar plates based on an independent set of whole-transcriptome analysis (Table 2). The seven genes are as follows: (i) *sfsA*, encoding a predicted maltose metabolism transcriptional regulator, (ii) *yfiA*, encoding the stationary-phase translation inhibitor and ribosome stability factor, (iii) *rpsV*, encoding the 30S ribosomal subunit protein, (iv) *dppA,* encoding the dipeptide transport protein and (v, vi, vii) three genes with unknown function, *ybiM*, *ydiZ* and *yjdN*. An insertion sequence element-interrupted Rac prophage *lom* homolog gene, *lomR*_1, was the only repressed gene identified by both sets of microarrays (Table 3). As none of the previously-characterized colanic acid generation genes were induced on deleting *yncC* in either set of DNA microarrays, YncC may regulate colanic acid production not at the transcription level but instead through an unknown indirect pathway.

YncC represses ybiM

The YncC protein sequence is conserved in *E. coli* strains, since BLAST analysis indicated that the 221 amino acid (aa) *E. coli* K-12 YncC shares 220 identical aa with the *E. coli* O157:H7 YncC (also 221 aa). Structure prediction analysis of YncC using ExPASy server (Gasteiger *et al*., 2003) suggested that YncC is a putative DNA-binding transcription regulator with a helix-turn-helix DNA-binding domain (aa 37–56). We suspected YncC directly binds to the promoter regions of some of the genes identified by the DNA microarrays and functions as an inducer or repressor to direct expression of these genes. Therefore, YncC binding of the promoter regions of the two most-induced genes in both glass wool and agar biofilm cells (*ybiM* and *sfsA*, Table 2), the two most-induced genes in glass wool biofilm cells (*ybeL* and *uspF*, Table 2), as well as with the one of the most repressed genes in glass wool biofilm cells (*yebT,* Table 3) was investigated using gel shift experiments. We were especially interested in *ybiM* and *yebT* since not only were they differentially expressed on *yncC* mutation but also both of them are regulated by AI-2 (DeLisa *et al*., 2001b; Wang *et al*., 2005). It was found that YncC binds to the promoter region of the *ybiM* gene (Figure 3a), but YncC did not bind under these conditions to the promoter regions of *ybeL*, *sfsA, uspF* and *yebT* (Figure 3b and data not shown). As DNA microarrays show that *ybiM* expression is induced 6.5-fold on deleting *yncC* (Table 2), this indicates that the putative transcription regulator YncC binds as a repressor of *ybiM*, which encodes a putative periplasmic protein with no known function.

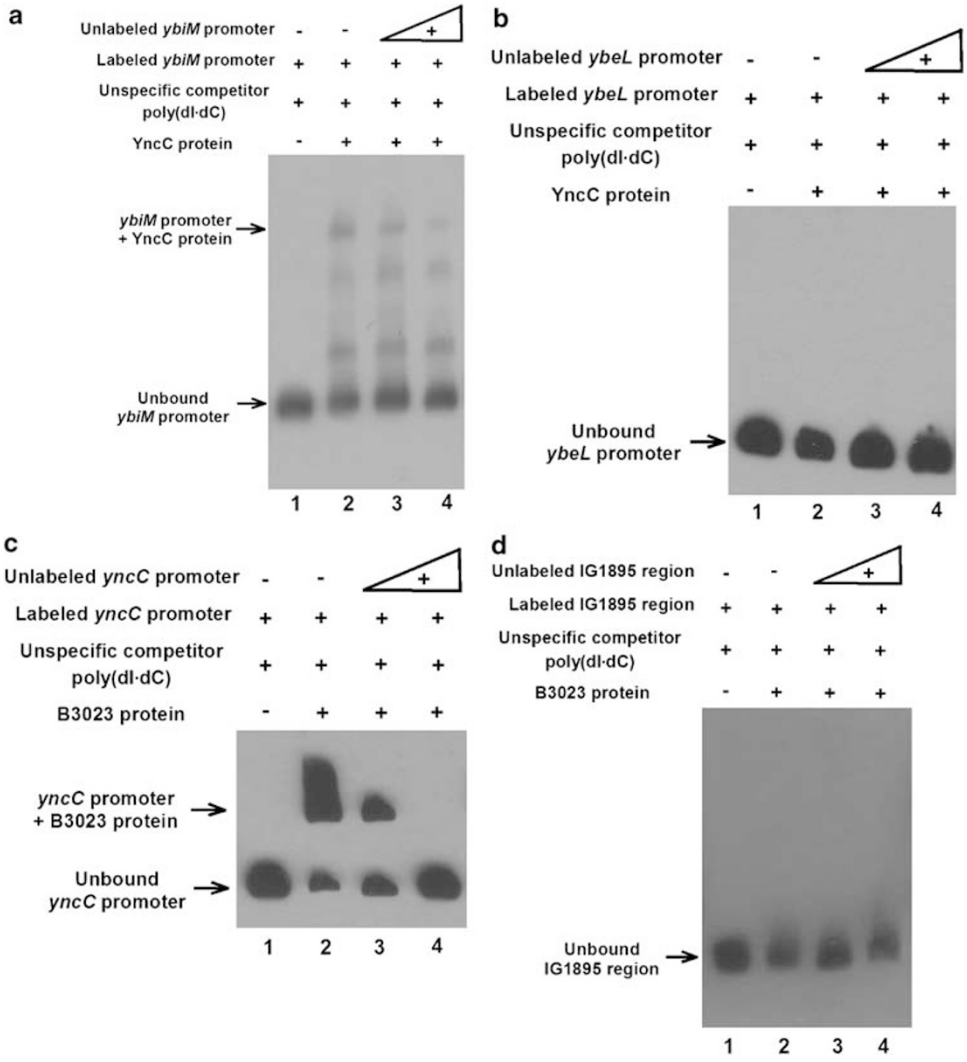

Figure 3 Electrophoretic mobility shift assay (EMSA) to test the binding of YncC to the *ybiM* promoter (**a**) and to the *ybeL* promoter (**b**), and binding of B3023 to the *ybeL* promoter (**c**) and to the IG1895 region (**d**). Lane 1: labeled promoter, lane 2: protein and labeled promoter, lane 3: protein, labeled promoter, and unlabeled promoter and lane 4: protein, labeled promoter, and increased unlabeled promoter. The triangle indicates that increasing amounts of unlabeled promoter were used as a specific competitor of the DNA–protein interaction. Each experiment was performed twice.

YncC regulates biofilm formation through ybiM

The poorly characterized YbiM belongs to the YhcN family of periplasmic proteins that includes BhsA; we found BhsA influences biofilm formation through hydrophobicity and stress response (Zhang *et al.*, 2007). In addition, earlier microarray analyses indicated that *ybiM* was induced 4.7-fold by the quorum-sensing signal AI-2 in *E. coli* K12 W3110 (DeLisa *et al.*, 2001b).

To investigate whether YncC regulates biofilm formation through *ybiM*, we constructed a MG1655 *yncC ybiM* double mutant. Biofilm formation of the MG1655 *yncC ybiM* double mutant in LB medium at 37 °C increased 2.3 ± 0.7-fold compared to the MG1655 *yncC* mutant. This indicates that the *ybiM* mutation represses the reduction seen in biofilm formation on deletion of *yncC*, which suggests that YncC influences biofilm formation most likely by regulating *ybiM* expression. In addition, the MG1655 *yncC ybiM* double mutant demonstrates the non-mucoid appearance of wild-type MG1655 (Figure 2a), which indicates again that the *ybiM* mutation represses phenotype seen with the *yncC* mutation. Consistently, colanic acid production of the MG1655 *yncC ybiM* double mutant was as low as the wild-type strain under the same conditions; that is, colanic acid production of the MG1655 *yncC ybiM* double mutant was decreased 173 ± 65-fold compared to the MG1655 *yncC* mutant. Corroborating the reduction in colanic acid, sensitivity to bacteriophage P1 infection for the MG1655 *yncC ybiM* double mutant increased 62 ± 27-fold compared to the MG1655 *yncC* mutant; hence, the double mutant was as sensitive to P1 as the wild-type strain. All these results indicate that YncC functions as the *ybiM* repressor and elicits its effect

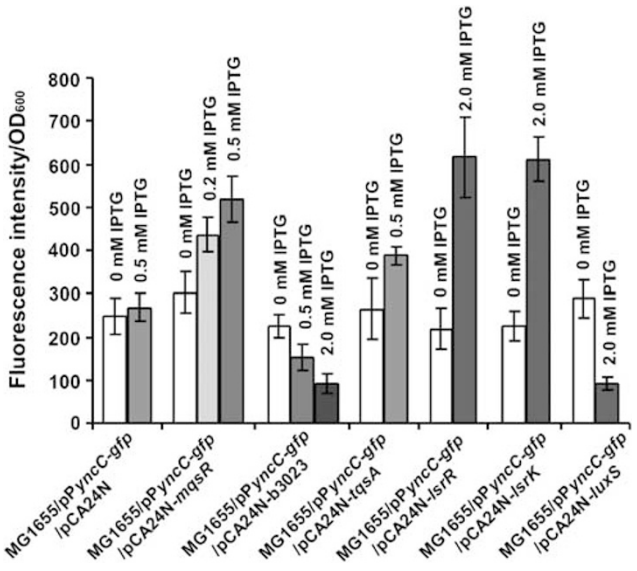

Figure 4 The GFP fluorescence intensity normalized with cell turbidity at 600 nm of MG1655/pP*yncC-gfp* overexpressing MqsR, B3023, TqsA, LsrR, LsrK or LuxS with IPTG induction from plasmid pCA24N-*mqsR*, pCA24N-b3023, pCA24N-*tqsA*, pCA24N-*lsrR*, pCA24N-*lsrK* or pCA24N-*luxS*, respectively. The experiments were repeated at least two times (one representative data set shown), and one s.d. is shown. GFP, green fluorescent protein; IPTG, isopropyl-β-D-thiogalactopyranoside.

on mucoidy and biofilm formation by regulating *ybiM*.

yncC *expression is influenced by MqsR, LsrR, LsrK, TqsA and YncC*

We also investigated the possibility that AI-2 regulates *yncC* expression as previous microarray analysis indicated that the *E. coli* quorum-sensing regulator MqsR induces *yncC* expression (González Barrios *et al.*, 2006). The effect of MqsR on *yncC* expression was quantified with a *yncC* promoter-*gfp* fusion (pP*yncC-gfp*) while overexpressing MqsR from pCA24N-*mqsR*. The specific GFP fluorescence intensity of MG1655/pP*yncC-gfp*/pCA24N-*mqsR* with 0.2 mM IPTG to induce *mqsR* increased 1.4 ± 0.2-fold compared to that without IPTG induction and increased 1.7 ± 0.2-fold with 0.5 mM IPTG induction (Figure 4); hence, MqsR induces *yncC* promoter activity, which is consistent with our previous microarray analysis that showed *yncC* expression is repressed on deleting *mqsR* (González Barrios *et al.*, 2006).

In a similar manner, we evaluated the effect of several other AI-2-related proteins on *yncC* expression, including LuxS (the AI-2 synthesis protein), LsrR (the repressor of the AI-2 uptake transporter complex), LsrK (cytoplasmic kinase, which phosphorylates AI-2 into an activated molecule inside *E. coli* cells) and TqsA (exporter of AI-2) (Figure 4). Adding 0.5 mM IPTG increased the specific GFP fluorescence intensity of MG1655/pP*yncC-gfp*/pCA24N-*lsrR* 2.7 ± 0.7-fold, increased the value of MG1655/pP*yncC-gfp*/pCA24N-*lsrK* 2.3 ± 0.5-fold, increased the value of MG1655/pP*yncC-gfp*/pCA24N-*tqsA* 1.5 ± 0.4-fold and decreased the value of MG1655/pP*yncC-gfp*/pCA24N-*luxS* 2.5 ± 0.6-fold (Figure 4). As a control, the presence of IPTG did not affect the value of the specific GFP fluorescence intensity of MG1655/pP*yncC-gfp*/pCA24N (empty vector control) (Figure 4). As additional negative controls, under the same test conditions, adding 0.5 mM IPTG to induce protein CRP or Crl did not significantly affect the value of the specific GFP fluorescence of the strain MG1655/pP*yncC-gfp*/pCA24N-*crp* or MG1655/pP*yncC-gfp*/pCA24N-*crl* (data not shown). Like YncC, both CRP and Crl are transcription regulatory proteins. These results indicate that LsrR, LsrK and TqsA induce *yncC* expression, whereas LuxS represses *yncC* expression.

The *yncC* promoter activities of wild-type *E. coli* MG1655 and the *E. coli* MG1655 *yncC* Km^R mutant were also evaluated by measuring the specific GFP fluorescence intensities of MG1655/pP*yncC-gfp* and MG1655 *yncC* Km^R/pP*yncC-gfp*. Under the same conditions, the specific GFP fluorescence intensity of MG1655 *yncC* Km^R/pP*yncC-gfp* was 2.0 ± 0.3-fold higher than that of MG1655/pP*yncC-gfp*, which indicates that YncC represses its own promoter activity.

Putative transcription regulator B3023 enhances MqsR toxicity and represses yncC

The quorum-sensing protein MqsR is a global regulator in *E. coli* (González Barrios *et al.*, 2006) and also elicits a toxic effect on *E. coli* growth (Shah *et al.*, 2006). We suspected that the upstream gene of *mqsR* (b3022), b3023, a putative transcription regulator, may be involved in regulation with MqsR so we examined the effect of deleting b3023 on the toxicity of MqsR by overexpressing MqsR via IPTG induction from plasmid pCA24N-*mqsR* in both *E. coli* MG1655 b3023 and wild-type MG1655. Without overexpressing MqsR, MG1655 b3023/pCA24N (empty vector) and MG1655/pCA24N exhibit similar growth (Figure 5); however, overexpressing MqsR with 2 mM IPTG decreases the growth of wild-type MG1655/pCA24N-*mqsR* by 9.3 ± 1.0-fold after 5 h (Figure 5). This confirms that MqsR has a toxic effect on MG1655. When overexpressing MqsR with 2 mM IPTG under the same conditions, the growth of MG1655 b3023/pCA24N-*mqsR* was only decreased by 2.2 ± 0.2-fold after 5 h, so the decrease was significantly reduced compared to MG1655/pCA24N-*mqsR* with 2 mM IPTG (Figure 5). This indicates that the b3023 mutation reduces the toxic effect of MqsR, which also supports our hypothesis that the putative transcription regulator B3023 may be involved in the MqsR (B3022) regulation pathway. This was further supported by the finding that deleting b3023 in *E. coli*

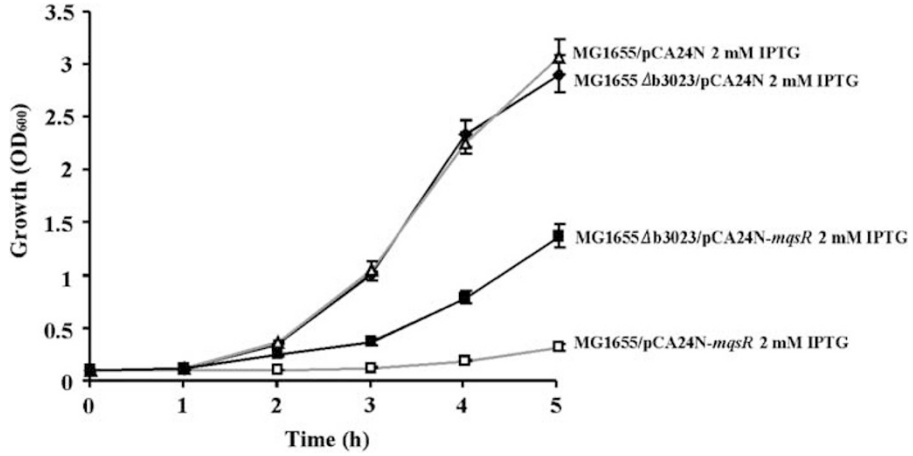

Figure 5 Impact of the Δb3023 mutation on the bacterial growth of MG1655 while overexpressing MqsR. MqsR was expressed from plasmid pCA24N-*mqsR* with 2 mM IPTG induction. Each experiment was performed in duplicate, and one s.d. is shown. IPTG, isopropyl-β-D-thiogalactopyranoside.

Table 4 List of gene candidates regulated by the putative transcription regulator B3023 identified *in vivo* using nickel-enrichment DNA microarrays

B3023 IG binding region	*IG-downstream gene*	*Enrichment (signal ratio of B3023:pBAD-Myc-His chip)*
IG_1895*	*ssrS* (b2911)	16.0
IG_2314*	*yiaT* (b3584) and *yiaU* (b3585)	19.7
IG_646	*yccT* (b0964) and *yccU* (b0965)	13.9
IG_108	*glnD* (b0167)	26.0
IG_543*	*rybA* (b4416) and *mntR* (b0817)	8.6
IG_1697	*pheA* (b2599)	16.0
IG_2395	*tnaA* (b3708)	10.6
IG_1551	*oxc* (b2373)	12.1
IG_2089	*ryhA* (b4450) and *yhbL* (b3209)	9.2
IG_1301	*yedQ* (b1956)	9.2
IG_1396	*yehS* (b2124)	16.0
IG_1297	*yodD* (b1953) and *dsrB* (b1952)	21.1
IG_953*	*yncC* (b1450)	14.9
IG_1382	*yegW*(b2101)	36.8
IG_934	*ydcH* (b1426)	10.6
IG_727	*ptsG*(b1101)	8.0

An asterisk indicates IG regions studied by a gel shift experiment with B3023.

K-12 BW25113 genetic background also similarly represses the toxic effect of MqsR (data not shown).

To determine what promoters B3023 binds *in vivo*, we used nickel-enrichment DNA microarrays and identified 16 IG regions that the putative transcription regulator B3023 may bind (Table 4). These results indicate that B3023 binds IG953 that includes the *yncC* gene upstream promoter region (enriched 15-fold); therefore, B3023 appears to regulate *yncC* expression. Interestingly, the 16 IG regions also include three regions covering small non-coding RNA (sRNA) and their upstream promoter regions: IG1895 covering sRNA *ssrS* (enriched 16-fold), which represses expression from sigma70-dependent promoters in the stationary phase (Wassarman and Storz, 2000), IG543 covering sRNA *rybA* (enriched 9-fold) and IG2089 covering sRNA *ryhA* (enriched 9-fold); *rybA* and *ryhA*, like other sRNA, may play important roles as regulators of translation and message stability (Gottesman, 2004).

We next tried to confirm the *in vitro* binding of B3023 with four IG regions by gel shift experiments including IG953 (including the *yncC* promoter), IG2314 (including the *yiaT* and *yiaU* promoters that were enriched 20-fold) and two sRNA IG regions (IG543 including sRNA *rybA*, and IG1895 including sRNA *ssrS*). Gel shift experiments clearly indicated that B3023 specifically binds to the *yncC* promoter under our test conditions (Figure 3c), but does not bind to the DNA fragments of the other three IG regions, IG2314, IG1895 and IG543, under the same conditions (Figure 3d and data not shown). This indicates that *yncC* expression is under the control of putative transcription regulator B3023, as predicted by the nickel-enrichment DNA microarrays.

To determine if the binding of B3023 regulates *yncC* expression as a repressor or inducer, we quantified *E. coli* MG1655 *yncC* promoter activity with specific GFP fluorescence intensity with a *yncC* promoter-*gfp* fusion via plasmid pP*yncC-gfp* while overexpressing B3023 via plasmid pCA24N-b3023 with IPTG induction. The specific GFP fluorescence intensity of MG1655/pP*yncC-gfp*/pCA24N-b3023 cells with 0.5 mM IPTG to induce B3023 decreased 1.5 ± 0.3-fold compared to that without IPTG induction and decreased 2.5 ± 0.7-fold with 2 mM IPTG induction (Figure 4). Hence, B3023 represses *yncC*.

Discussion

Previous research showed the cross-species bacterial communication quorum-sensing signal AI-2 stimulates *E. coli* biofilm by stimulating motility genes, and this effect is mediated by MqsR, which then regulates QseBC (González Barrios *et al.*, 2006). In this study, by investigating the biofilm changes caused by mutating the transcription regulator YncC, by investigating the genes regulated by YncC via DNA microarrays, by investigating which promoters are directly bound by YncC using gel shift experiments and by investigating which proteins affect *yncC* expression, we demonstrate that MqsR-regulated YncC influences biofilm formation and mucoidy by repressing expression of the periplasmic protein YbiM. We also demonstrate B3023 regulates *yncC* as a repressor.

YbiM belongs to the YhcN family, which has nine paralogous, low-molecular-weight proteins: BhsA (Zhang *et al.*, 2007), YahO, YbiJ, YbiM, YdgH, YhcN, YjfN, YjfO and YjfY in *E. coli* (Rudd *et al.*, 1998). Sharing a predicted signal peptide in the N-terminus and a common motif in the C-terminus with unknown function (TAXIYK, where A and Y are conserved for all nine proteins and X represents any aa), the YhcN family of proteins were proposed to interact functionally and/or structurally with each other, to have evolved from a common ancestor, and to play roles in self-identification or colony organization by cell-cell contact or intercellular signaling (Rudd *et al.*, 1998). We demonstrated that one of the YhcN family proteins, BhsA (YcfR), influences biofilm formation through hydrophobicity and stress response (Zhang *et al.*, 2007). Here, we demonstrate that another YhcN family member, YbiM, is regulated by YncC, and that YbiM affects both biofilm formation and mucoidy. Apart from BhsA and YbiM, the functions of the other members of this family remain unknown, so whether they are related to biofilm formation deserves to be investigated as a means to discover the role of this protein family in biofilm development.

E. coli produces different types of EPS including serotype-specific lipopolysaccharide O-antigen, capsular K-antigen, colanic acid, (1→4)-β-glucan cellulose and (1→6)-β-*N*-acetylglucosamine polymer, which play important roles in the interaction between the bacterium and its environment (Ferrieres *et al.*, 2007). The precise role of the EPS in bacteria is dependent on the natural environment of the microorganism (Kumar *et al.*, 2007). In *E. coli*, overexpressing the genes involved in colanic acid synthesis, such as *djlA* and *rcsF*, induces colanic acid overproduction and elicits mucoidy (Genevaux *et al.*, 2001; Potrykus and Wegrzyn, 2004). Here, we demonstrate that the *yncC* mutation leads to overproduction of colanic acid and so elicits mucoidy, and at the same time represses biofilm formation. Colanic acid is critical for the formation of the complex three-dimensional structure and depth of *E. coli* biofilms, while is not required for surface attachment (Danese *et al.*, 2000). In contrast, recent research indicates that overproduced *E. coli* colanic acid blocks the time-dependent adhesion of bacteria to both hydrophilic and hydrophobic surfaces (Hanna *et al.*, 2003). So, most likely the *yncC* mutation represses *E. coli* biofilm formation at the early stage by abnormally overproducing colanic acid, which blocks bacterial attachment. Consistent with our results, the quorum-sensing-impaired mutant of the phytopathogenic bacterium *Pantoea stewartii* subsp. *stewartii* elicits hypermucoidy and EPS-overproduction with the result that it attaches poorly to surfaces and forms poor biofilms (Koutsoudis *et al.*, 2006).

As EPS can mask bacteriophage receptors on bacterial surfaces to block phage infection (Forde and Fitzgerald, 2003), we suspected that the overproduction of colanic acid caused by the *yncC* mutation may also mask unknown signal receptors on the bacterial cell surface to block bacterial cell communication and then biofilm formation. Since deleting *yncC* did not cause differential expression of previously characterized colanic acid generation genes, *yncC* may regulate colanic acid production not at the transcription level but instead through an unknown indirect pathway that includes the periplasmic protein YbiM and/or other structural proteins on the bacterial cell surface.

E. coli MqsR is a small protein (98 aa), which has homologs in several other genera including *Yersinia*, *Cupriavidus*, *Burkholderia*, *Xylella*, *Bordetella*, *Polaromonas*, *Pseudomonas*, *Nitrosospira* and *Ralstonia* based on sequence similarity. However, MqsR has only been characterized in *E. coli*. In *E. coli*, MqsR is a global regulator of gene expression (González Barrios *et al.*, 2006) and is a toxin protein (Shah *et al.*, 2006; Figure 5), which has been suggested to selectively target DNA gyrase or topoisomerase (Shah *et al.*, 2006). This raises the possibility that MqsR may elicit its global regulation effect on gene expression by affecting bacterial DNA tertiary structure. The genes regulated by MqsR include *lsrK*, encoding a cytoplasmic kinase that phosphorylates AI-2 into an activated molecule inside *E. coli* cells, and *glpDFK*, encoding a glycerol uptake and metabolism system that regulates AI-2 uptake and *lsr* operon transcription through cyclic AMP-catabolite activator protein-dependent regulation (Taga *et al.*, 2003; Xavier and Bassler, 2005; González Barrios *et al.*, 2006). This suggests that signal AI-2 not only stimulates biofilm formation through MqsR as indicated before (González Barrios *et al.*, 2006), but also that AI-2 uptake and internalization is regulated by MqsR. Since no DNA-binding transcription regulator domain or other previous well characterized functional domain was predicted for MqsR, this suggests MqsR regulates the expression of genes, including these AI-2 related *lsrK* and *glpDFK* genes, through an unknown mechanism. The putative transcription

regulator YncC we characterized here most likely is involved in this process.

We investigated the effect of the quorum-sensing signal AI-2 on *yncC* expression; however, under our test conditions, addition of exogenous AI-2 (Omm Scientific Inc., Dallas, TX, USA) did not significantly change *yncC* expression in MG1655 or in the MG1655 *luxS* Km^R mutant. In contrast, overexpressing LuxS repressed *yncC* expression (Figure 4), and deleting *luxS* significantly increased *yncC* expression in MG1655 (1.3 ± 0.1-fold). Since YncC represses *ybiM*, this also suggests that overexpression of LuxS can induce *ybiM* expression. This agrees with the previous finding that AI-2 induces *ybiM* expression (DeLisa *et al.*, 2001b). Together, these results raise the possibility LuxS and its signal AI-2 may regulate *yncC* and *ybiM* through both metabolic and signaling pathways.

Overexpressing the AI-2 exporter TqsA, *lsr*-operon regulators LsrR and LsrK, and quorum-sensing regulator MqsR induced *yncC* expression. Whether these induction effects are by derepressing *yncC* expression via its repressor B3023 and how these effects are related to *yncC* negative self-regulation needs to be investigated further. For all of these tests, *yncC* expression levels were measured when bacterial cells were grown into the stationary phase after 6-h incubation in LB medium at 37 °C since internalization of AI-2 takes place in the stationary phase (Xavier and Bassler, 2005). Moreover, MG1655 *yncC* and MG1655 have the same specific growth rate during the early exponential phase, but obtain different cell densities at the late exponential stage and stationary stage (the *yncC* mutant enters stationary stage with a significantly lower cell density, turbidity of 600 nm of 2.7 ± 0.2 vs 5.3 ± 0.1 for the wild-type strain). This suggests YncC functions at the late exponential stage and stationary stage, which are consistent with the finding that the homolog of *E. coli yncC* in the Gram-negative bacterium *Salmonella enterica* serovar typhimurium is under the regulation of the stationary-phase sigma factor σ^S (RpoS) (Ibanez-Ruiz *et al.*, 2000). This mimics bacterial AI-2 internalization behavior (Xavier and Bassler, 2005) and also agrees with the concept that RpoS is intimately associated with *E. coli* quorum sensing (DeLisa *et al.*, 2001a), which suggests that the quorum-sensing process, stress response process and biofilm development are tightly linked.

This study reveals that the MqsR-regulated *yncC* gene is important for biofilm formation, and that YncC regulates *E. coli* biofilm formation and mucoidy via colanic acid production by repressing expression of *ybiM*, which encodes a putative periplasmic protein. Further characterization of B3023 and YbiM may link bacterial signaling pathways with biofilm formation. We propose *yncC* should be named *mcbR* (MqsR-controlled colanic acid and biofilm regulator), and *ybiM*, the first gene regulated by *mcbR*, should be *mcbA*. A conceptual model of how *yncC* and AI-2 influence biofilm formation is shown in Figure 6.

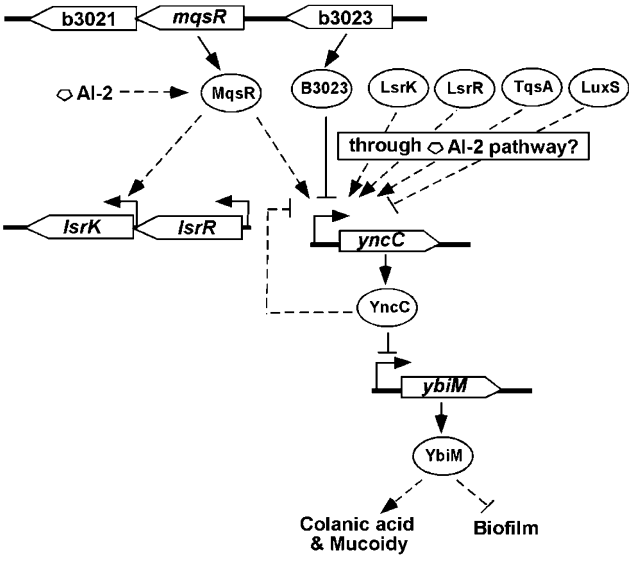

Figure 6 Conceptual model for *yncC* regulation of biofilm formation. → indicates induction; ⊥ indicates repression; dashed lines indicate indirect regulation and solid lines indicate direct regulation.

Acknowledgements

This research was supported by the NIH (EB003872-01A1). We thank Proffesor Steven Lindow for providing plasmid pPROBE-*gfp*[tagless] and the National of Institute of Genetics for the KEIO and ASKA clones.

References

Andrews SC, Berks BC, McClay J, Ambler A, Quail MA, Golby P *et al.* (1997). A 12-cistron *Escherichia coli* operon (*hyf*) encoding a putative proton-translocating formate hydrogenlyase system. *Microbiology* **143**: 3633–3647.

Baba T, Ara T, Hasegawa M, Takai Y, Okumura Y, Baba M *et al.* (2006). Construction of *Escherichia coli* K-12 in-frame, single-gene knockout mutants: the Keio collection. *Mol Syst Biol* **2**: 2006.0008.

Bansal T, Englert D, Lee J, Hegde M, Wood TK, Jayaraman A. (2007). Differential effects of epinephrine, norepinephrine, and indole on *Escherichia coli* O157:H7 chemotaxis, colonization, and gene expression. *Infect Immun* **75**: 4597–4607.

Beloin C, Valle J, Latour-Lambert P, Faure P, Kzreminski M, Balestrino D *et al.* (2004). Global impact of mature biofilm lifestyle on *Escherichia coli* K-12 gene expression. *Mol Microbiol* **51**: 659–674.

Benjamini Y, Hochberg Y. (1995). Controlling the false discovery rate: a practical and powerful approach to multiple testing. *J Royal Stat Soc B* **57**: 289–300.

Blattner FR, Plunkett 3rd G, Bloch CA, Perna NT, Burland V, Riley M *et al.* (1997). The complete genome sequence of *Escherichia coli* K-12. *Science* **277**: 1453–1474.

Camilli A, Bassler BL. (2006). Bacterial small-molecule signaling pathways. *Science* **311**: 1113–1116.

Cherepanov PP, Wackernagel W. (1995). Gene disruption in *Escherichia coli*: Tc^R and Km^R cassettes with the option of Flp-catalyzed excision of the antibiotic-resistance determinant. *Gene* **158**: 9–14.

Claret L, Hughes C. (2002). Interaction of the atypical prokaryotic transcription activator FlhD2C2 with early promoters of the flagellar gene hierarchy. *J Mol Biol* **321**: 185–199.

Clarke MB, Sperandio V. (2005). Transcriptional regulation of *flhDC* by QseBC and sigma (FliA) in enterohaemorrhagic *Escherichia coli*. *Mol Microbiol* **57**: 1734–1749.

Da Re S, Ghigo JM. (2006). A CsgD-independent pathway for cellulose production and biofilm formation in *Escherichia coli*. *J Bacteriol* **188**: 3073–3087.

Danese PN, Pratt LA, Kolter R. (2000). Exopolysaccharide production is required for development of *Escherichia coli* K-12 biofilm architecture. *J Bacteriol* **182**: 3593–3596.

Danese PN, Silhavy TJ. (1998). CpxP, a stress-combative member of the Cpx regulon. *J Bacteriol* **180**: 831–839.

Datsenko KA, Wanner BL. (2000). One-step inactivation of chromosomal genes in *Escherichia coli* K-12 using PCR products. *Proc Natl Acad Sci USA* **97**: 6640–6645.

DeLisa MP, Valdes JJ, Bentley WE. (2001a). Mapping stress-induced changes in autoinducer AI-2 production in chemostat-cultivated *Escherichia coli* K-12. *J Bacteriol* **183**: 2918–2928.

DeLisa MP, Wu CF, Wang L, Valdes JJ, Bentley WE. (2001b). DNA microarray-based identification of genes controlled by autoinducer 2-stimulated quorum sensing in *Escherichia coli*. *J Bacteriol* **183**: 5239–5247.

Domka J, Lee J, Bansal T, Wood TK. (2007). Temporal gene-expression in *Escherichia coli* K-12 biofilms. *Environ Microbiol* **9**: 332–346.

Domka J, Lee J, Wood TK. (2006). YliH (BssR) and YceP (BssS) regulate *Escherichia coli* K-12 biofilm formation by influencing cell signaling. *Appl Environ Microbiol* **72**: 2449–2459.

Edgar R, Domrachev M, Lash AE. (2002). Gene expression omnibus: NCBI gene expression and hybridization array data repository. *Nucleic Acids Res* **30**: 207–210.

Ferrieres L, Aslam SN, Cooper RM, Clarke DJ. (2007). The *yjbEFGH* locus in *Escherichia coli* K-12 is an operon encoding proteins involved in exopolysaccharide production. *Microbiology* **153**: 1070–1080.

Forde A, Fitzgerald GF. (2003). Molecular organization of exopolysaccharide (EPS) encoding genes on the lactococcal bacteriophage adsorption blocking plasmid, pCI658. *Plasmid* **49**: 130–142.

Gasteiger E, Gattiker A, Hoogland C, Ivanyi I, Appel RD, Bairoch A. (2003). ExPASy: The proteomics server for in-depth protein knowledge and analysis. *Nucleic Acids Res* **31**: 3784–3788.

Genevaux P, Wawrzynow A, Zylicz M, Georgopoulos C, Kelley WL. (2001). DjlA is a third DnaK co-chaperone of *Escherichia coli*, and DjlA-mediated induction of colanic acid capsule requires DjlA-DnaK interaction. *J Biol Chem* **276**: 7906–7912.

González Barrios AF, Zuo R, Hashimoto Y, Yang L, Bentley WE, Wood TK. (2006). Autoinducer 2 controls biofilm formation in *Escherichia coli* through a novel motility quorum-sensing regulator (MqsR, B3022). *J Bacteriol* **188**: 305–316.

Gordon JJ, Towsey MW, Hogan JM, Mathews SA, Timms P. (2006). Improved prediction of bacterial transcription start sites. *Bioinformatics* **22**: 142–148.

Gottesman S. (2004). The small RNA regulators of *Escherichia coli*: roles and mechanisms. *Annu Rev Microbiol* **58**: 303–328.

Hancock V, Klemm P. (2007). Global gene expression profiling of asymptomatic bacteriuria *Escherichia coli* during biofilm growth in human urine. *Infect Immun* **75**: 966–976.

Hanna A, Berg M, Stout V, Razatos A. (2003). Role of capsular colanic acid in adhesion of uropathogenic *Escherichia coli*. *Appl Environ Microbiol* **69**: 4474–4481.

Herzberg M, Kaye IK, Peti W, Wood TK. (2006). YdgG (TqsA) controls biofilm formation in *Escherichia coli* K-12 through autoinducer 2 transport. *J Bacteriol* **188**: 587–598.

Ho TD, Waldor MK. (2007). Enterohemorrhagic *Escherichia coli* O157:H7 gal mutants are sensitive to bacteriophage P1 and defective in intestinal colonization. *Infect Immun* **75**: 1661–1666.

Ibanez-Ruiz M, Robbe-Saule V, Hermant D, Labrude S, Norel F. (2000). Identification of RpoS (σ^S)-regulated genes in *Salmonella enterica* serovar typhimurium. *J Bacteriol* **182**: 5749–5756.

Jackson DW, Simecka JW, Romeo T. (2002). Catabolite repression of *Escherichia coli* biofilm formation. *J Bacteriol* **184**: 3406–3410.

Jeon B, Itoh K, Misawa N, Ryu S. (2003). Effects of quorum sensing on *flaA* transcription and autoagglutination in *Campylobacter jejuni*. *Microbiol Immunol* **47**: 833–839.

Keseler IM, Collado-Vides J, Gama-Castro S, Ingraham J, Paley S, Paulsen IT *et al.* (2005). EcoCyc: a comprehensive database resource for *Escherichia coli*. *Nucleic Acids Res* **33**: D334–D337.

Koutsoudis MD, Tsaltas D, Minogue TD, von Bodman SB. (2006). Quorum-sensing regulation governs bacterial adhesion, biofilm development, and host colonization in *Pantoea stewartii* subspecies *stewartii*. *Proc Natl Acad Sci USA* **103**: 5983–5988.

Kumar AS, Mody K, Jha B. (2007). Bacterial exopolysaccharides—a perception. *J Basic Microbiol* **47**: 103–117.

Lee J, Bansal T, Jayaraman A, Bentley WE, Wood TK. (2007a). Enterohemorrhagic *Escherichia coli* biofilms are inhibited by 7-hydroxyindole and stimulated by isatin. *Appl Environ Microbiol* **73**: 4100–4109.

Lee J, Jayaraman A, Wood TK. (2007b). Indole is an inter-species biofilm signal mediated by SdiA. *BMC Microbiol* **7**: 42.

Lee J, Page R, García-Contreras R, Palermino JM, Zhang XS, Doshi O *et al.* (2007c). Structure and function of the *Escherichia coli* protein YmgB: a protein critical for biofilm formation and acid-resistance. *J Mol Biol* **373**: 11–26.

Li J, Attila C, Wang L, Wood TK, Valdes JJ, Bentley WE. (2007). Quorum sensing in *E. coli* is signaled by AI-2/LsrR: effects on sRNA and biofilm architecture. *J Bacteriol* **189**: 6011–6020.

Liu X, Matsumura P. (1994). The FlhD/FlhC complex, a transcriptional activator of the *Escherichia coli* flagellar class II operons. *J Bacteriol* **176**: 7345–7351.

Lombardia E, Rovetto AJ, Arabolaza AL, Grau RR. (2006). A LuxS-dependent cell-to-cell language regulates social behavior and development in *Bacillus subtilis*. *J Bacteriol* **188**: 4442–4452.

Mendrygal KE, González JE. (2000). Environmental regulation of exopolysaccharide production in *Sinorhizobium meliloti*. *J Bacteriol* **182**: 599–606.

Miller WG, Leveau JH, Lindow SE. (2000). Improved *gfp* and *inaZ* broad-host-range promoter-probe vectors. *Mol Plant Microbe Interact* **13**: 1243–1250.

Obadia B, Lacour S, Doublet P, Baubichon-Cortay H, Cozzone AJ, Grangeasse C. (2007). Influence of tyrosine-kinase Wzc activity on colanic acid production in *Escherichia coli* K12 cells. *J Mol Biol* **367**: 42–53.

Ogino T, Matsubara M, Kato N, Nakamura Y, Mizuno T. (1998). An *Escherichia coli* protein that exhibits phosphohistidine phosphatase activity towards the HPt domain of the ArcB sensor involved in the multistep His-Asp phosphorelay. *Mol Microbiol* **27**: 573–585.

Otto K, Silhavy TJ. (2002). Surface sensing and adhesion of *Escherichia coli* controlled by the Cpx-signaling pathway. *Proc Natl Acad Sci USA* **99**: 2287–2292.

Petty NK, Evans TJ, Fineran PC, Salmond GP. (2007). Biotechnological exploitation of bacteriophage research. *Trends Biotechnol* **25**: 7–15.

Postma PW, Lengeler JW, Jacobson GR. (1993). Phosphoenolpyruvate:carbohydrate phosphotransferase systems of bacteria. *Microbiol Rev* **57**: 543–594.

Potrykus J, Wegrzyn G. (2004). The *ypdI* gene codes for a putative lipoprotein involved in the synthesis of colanic acid in *Escherichia coli*. *FEMS Microbiol Lett* **235**: 265–271.

Pratt LA, Kolter R. (1998). Genetic analysis of *Escherichia coli* biofilm formation: roles of flagella, motility, chemotaxis and type I pili. *Mol Microbiol* **30**: 285–293.

Puan KJ, Wang H, Dairi T, Kuzuyama T, Morita CT. (2005). *fldA* is an essential gene required in the 2-C-methyl-D-erythritol 4-phosphate pathway for isoprenoid biosynthesis. *FEBS Lett* **579**: 3802–3806.

Qiu D, Eisinger VM, Rowen DW, Yu HD. (2007). Regulated proteolysis controls mucoid conversion in *Pseudomonas aeruginosa*. *Proc Natl Acad Sci USA* **104**: 8107–8112.

Rader BA, Campagna SR, Semmelhack MF, Bassler BL, Guillemin K. (2007). The quorum sensing molecule AI-2 regulates motility and flagellar morphogenesis in *Helicobacter pylori*. *J Bacteriol* **189**: 6109–6117.

Reed JL, Vo TD, Schilling CH, Palsson BO. (2003). An expanded genome-scale model of *Escherichia coli* K-12 (iJR904 GSM/GPR). *Genome Biol* **4**: R54. 1–R54.12.

Ren D, Bedzyk LA, Thomas SM, Ye RW, Wood TK. (2004a). Gene expression in *Escherichia coli* biofilms. *Appl Microbiol Biotechnol* **64**: 515–524.

Ren D, Bedzyk LA, Ye RW, Thomas SM, Wood TK. (2004b). Differential gene expression shows natural brominated furanones interfere with the autoinducer-2 bacterial signaling system of *Escherichia coli*. *Biotechnol Bioeng* **88**: 630–642.

Ren D, Zuo R, González Barrios AF, Bedzyk LA, Eldridge GR, Pasmore ME *et al.* (2005). Differential gene expression for investigation of *Escherichia coli* biofilm inhibition by plant extract ursolic acid. *Appl Environ Microbiol* **71**: 4022–4034.

Rickard AH, Palmer Jr RJ, Blehert DS, Campagna SR, Semmelhack MF, Egland PG *et al.* (2006). Autoinducer 2: a concentration-dependent signal for mutualistic bacterial biofilm growth. *Mol Microbiol* **60**: 1446–1456.

Rudd KE, Humphery-Smith I, Wasinger VC, Bairoch A. (1998). Low molecular weight proteins: a challenge for post-genomic research. *Electrophoresis* **19**: 536–544.

Sambrook J, Fritsch EF, Maniatis T. (1989). *Molecular Cloning, A Laboratory Manual*. Cold Spring Harbor Laboratory Press: Cold Spring Harbor, NY.

Schauder S, Shokat K, Surette MG, Bassler BL. (2001). The LuxS family of bacterial autoinducers: biosynthesis of a novel quorum-sensing signal molecule. *Mol Microbiol* **41**: 463–476.

Schembri MA, Kjaergaard K, Klemm P. (2003). Global gene expression in *Escherichia coli* biofilms. *Mol Microbiol* **48**: 253–267.

Shah D, Zhang Z, Khodursky A, Kaldalu N, Kurg K, Lewis K. (2006). Persisters: a distinct physiological state of *E. coli*. *BMC Microbiol* **6**: 53.

Shao H, Lamont RJ, Demuth DR. (2007). Autoinducer-2 is required for biofilm growth of *Aggregatibacter* (*Actinobacillus*) *actinomycetemcomitans*. *Infect Immun* **75**: 4211–4218.

Stanley NR, Lazazzera BA. (2004). Environmental signals and regulatory pathways that influence biofilm formation. *Mol Microbiol* **52**: 917–924.

Stevenson G, Andrianopoulos K, Hobbs M, Reeves PR. (1996). Organization of the *Escherichia coli* K-12 gene cluster responsible for production of the extracellular polysaccharide colanic acid. *J Bacteriol* **178**: 4885–4893.

Taga ME, Miller ST, Bassler BL. (2003). Lsr-mediated transport and processing of AI-2 in *Salmonella typhimurium*. *Mol Microbiol* **50**: 1411–1427.

Taga ME, Semmelhack JL, Bassler BL. (2001). The LuxS-dependent autoinducer AI-2 controls the expression of an ABC transporter that functions in AI-2 uptake in *Salmonella typhimurium*. *Mol Microbiol* **42**: 777–793.

Tamimi Y, Lines M, Coca-Prados M, Walter MA. (2004). Identification of target genes regulated by FOXC1 using nickel agarose-based chromatin enrichment. *Invest Ophthalmol Vis Sci* **45**: 3904–3913.

Van Houdt R, Michiels CW. (2005). Role of bacterial cell surface structures in *Escherichia coli* biofilm formation. *Res Microbiol* **156**: 626–633.

Wang L, Li J, March JC, Valdes JJ, Bentley WE. (2005). *luxS*-dependent gene regulation in *Escherichia coli* K-12 revealed by genomic expression profiling. *J Bacteriol* **187**: 8350–8360.

Wassarman KM, Storz G. (2000). 6S RNA regulates *E. coli* RNA polymerase activity. *Cell* **101**: 613–623.

Wheeler DL, Barrett T, Benson DA, Bryant SH, Canese K, Chetvernin V *et al.* (2006). Database resources of the national center for biotechnology information. *Nucleic Acids Res* **34**: D173–D180.

Wiame E, Delpierre G, Collard F, Van Schaftingen E. (2002). Identification of a pathway for the utilization of the Amadori product fructoselysine in *Escherichia coli*. *J Biol Chem* **277**: 42523–42529.

Xavier KB, Bassler BL. (2003). LuxS quorum sensing: more than just a numbers game. *Curr Opin Microbiol* **6**: 191–197.

Xavier KB, Bassler BL. (2005). Regulation of uptake and processing of the quorum-sensing autoinducer AI-2 in *Escherichia coli*. *J Bacteriol* **187**: 238–248.

Zhang XS, García-Contreras R, Wood TK. (2007). YcfR (BhsA) influences *Escherichia coli* biofilm formation through stress response and surface hydrophobicity. *J Bacteriol* **189**: 3051–3062.

Zinkewich-Peotti K, Fraser JM. (1988). New locus for exopolysaccharide overproduction in *Escherichia coli* K-12. *J Bacteriol* **170**: 1405–1407.